A Numerical Study of the Track-Seeking Dynamics of the 30% *TNPS* and *U* Sliders on Smooth and Laser-Textured Disks

Liangsheng Chen

David B. Bogy

Computer Mechanics Lab

University of California at Berkeley

June 1998

Contents

List of Tables

List of Figures

Abstract

In this report, we studied the track-seeking dynamics of two "pico" sliders, namely, the TNPS and U sliders, using the CML's air bearing dynamic simulator. The two sliders are found to have distinct dynamic characteristics. The air bearing of the U slider is stiffer than that of the TNPS slider and has smaller damping ratios. During track-seeking, the spacing change of the U slider is significantly larger than that of the TNPS slider. An increase in the seeking acceleration leads to more significant inertial effects and larger spacing change. When the sliders move off the laser texture zone to the smooth zone there is a roll angle change. The higher the laser bumps, the larger the roll angle increase. Since the air bearing of the U slider is stiffer than that of the TNPS slider, the roll angle change is smaller. The overall track-seeking performance of the TNPS slider is better than that of the U slider.

1 Introduction

In magnetic hard disk drives, track-seeking is the process for the slider to move from one track to another. During this process, the head/disk spacing changes as a result of the change of the skew angle and the relative disk velocity, as well as the inertia force due to the slider's acceleration or deceleration in the cross track direction. Track access time is one of the important hard drive performance indices. Increasing the seeking acceleration can reduce the access time. Meanwhile it also leads to larger inertial effects and adversely affects the head/disk spacing. One of the concerns in slider design is the impact of the flying height change on drive reliability. This is especially of concern for drives of less than 2 micro-inch flying height and drives with MR heads. Different ABS designs can perform quite differently during the track-seeking process. Therefore, a study of the track-seeking dynamics should help to improve the ABS design to achieve better track-seeking performance.

Berg and Buettner [1] studied the inertial, viscous and relative head/disk velocity on head/disk spacing changes during track accessing for a "nano" slider with tri-rails. Cha et al. [2] looked into the head/disk spacing changes during seek operation for TPC sliders. They used a quasi-static approach to numerically simulate the track-seeking and found that at high seek velocities the skew angle effect dominates over the inertia effect. Liu and Soh [3] experimentally investigated the effects of seeking-velocity on air bearing skew angle, air flow speed and flying performance of TPC and Tri-pad sliders. They, too, did not consider the effects of the slider's inertia and acceleration due to the difficulty of measuring flying height during track-seeking with the commercially available dynamic flying height tester.

Compared to nano (2 mm X 1.6 mm) sliders, the pico (1.2 mm X 1.0 mm) sliders have several significant technical advantages, including improved seek performance and shock performance, improved merge clearances (allowing tighter disk/disk spacing), better head/disk compliance and improved head/media tribology (lower stiction, friction and wear) [4]. It is estimated that about half of the sliders in drives will be pico heads by the end of 1998. Pico sliders, however, are inherently more sensitive to forces exerted by the suspension and

disk than nano sliders. In our study, using the CML's air bearing dynamic simulator [5], we first compared the track-seeking performance of two pico sliders on a smooth disk surface. Then we studied the effect of seeking acceleration on the spacing change of the TNPS slider. Finally we investigated the dynamics of the two pico sliders during transition on and off of a laser texture zone.

2 Theoretical Models and Numerical Methods

2.1 Air Bearing Model

The pressure distribution between the slider and the rotating disk can be described by the compressible Reynolds equation. The generalized Reynolds equation written in the non-dimensionalized form is as follows:

$$\frac{\partial}{\partial X}[\hat{Q}PH^3\frac{\partial P}{\partial X} - \Lambda_X PH] + \frac{\partial}{\partial Y}[\hat{Q}PH^3\frac{\partial P}{\partial Y} - \Lambda_Y PH] = \sigma\frac{\partial}{\partial T}[PH], \tag{1}$$

where, $\Lambda_X = 6\mu UL/p_a h_m^2$ and $\Lambda_Y = 6\mu VL/p_a h_m^2$ are the bearing numbers in the x and y directions, $\sigma = 12\mu\omega L^2/p_a h_m^2$ is the squeeze number, μ is the viscosity, p_a is the ambient pressure, and $\hat{Q}$ is the Poiseuille flow factor.

2.2 Air Bearing Slider and Suspension Dynamics

The motion of an air bearing slider flying over a rotating disk is described by:

$$\begin{aligned} m\ddot{z} &= F + \int_A (p - p_a)dA \\ I_\theta\ddot{\theta} &= M_\theta + \int_A (p - p_a)(x_g - x)dA \\ I_\phi\ddot{\phi} &= M_\phi + \int_A (p - p_a)(y_g - y)dA, \end{aligned} \tag{2}$$

where, z, θ, ϕ are the vertical displacement, pitch and roll, respectively. I_θ, I_ϕ are moments of inertia, x_g, y_g are the positions of the slider's center of gravity, and F, M_θ, M_ϕ are the

force and moments exerted on the slider by the suspension. For track-seeking, M_θ, M_ϕ include the contribution of the inertial forces.

A modal truncation method [7] is applied to model the suspension dynamics during track-seeking. The finite element code ABAQUS is used for the modal analysis of the suspension. The first 10 modes are extracted and a linear combination of them is used to represent the suspension dynamics.

2.3 Numerical Methods

The dynamic analysis of a slider flying over a rotating disk requires simultaneous solution of equations (1)-(2) and the dynamics of the suspension. The generalized Reynolds equation (1) is discretized using Patankar's control volume method [7] [8] and solved using the alternating direction line sweeping method combined with a multi-grid method [9] [10]. The coupled equations are solved using the Newmark-β method [11].

3 Results and Discussion

3.1 Dynamic Characteristics of the TNPS and U Sliders

As shown in Figure 1(a), the 30% TNPS slider consists of transverse pressure contour (TPC) outer rails with a recess depth of 0.432 μm, two full-length pressure relief slots with a recess depth of 3.332 μm, and a central sub-ambient "negative" pressure (NP) cavity with a recess depth of 2.9 μm. The TNPS slider thus has desired features of both the TPC and NP sliders. The pressure relief slots can prevent the convection of air bearing pressure among different component surfaces and hence reduce the pressure distortion and dilution [12]. The slider has a crown of 20.32 nm. Figure 1(b) shows its air bearing pressure profile when flying at a disk radius of 20.5 mm. The disk speed is 7200 rpm and the suspension pre-load is 2.5g. The 30% U slider, as shown in Figure 2(a), is a straight-railed negative pressure slider with a recess depth of 3.556 μm and a crown of 20.32 nm. Its air bearing pressure profile is shown

in Figure 2(b). Table 1 summarizes the flying attitudes of the two sliders.

In a previous study [13], using a modal analysis software developed at CML [6], we calculated the air bearing stiffness, natural frequencies and damping ratios from the sliders' impulse responses. For convenience, we include the results here in Tables 2, 3 and 4. Please note that in Tables 3 and 4, mode 1 is mainly in pitch motion with the modal line near the trailing edge for both sliders, while mode 2 of the TNPS slider and mode 3 of the U slider are mainly in the roll motion. From Table 2 we can see that the air bearing of the U slider is stiffer than that of the TNPS slider because the former has a large negative pressure cavity. A high air bearing stiffness is usually desirable because the air bearing stiffness gives a measure of the stability and control that can be expected from the HDI when the slider is subjected to dynamic input.

The damping of the air bearing of a slider is caused by the viscous dissipation of energy on the slider ABS. From Table 4 we can see that the air bearing of the U slider has smaller damping, which is attributed to its rail shape since it has few "outlets" to dissipate energy. On the contrary, the TPC section of the TNPS slider leads to much higher damping.

3.2 Track-seeking on a Smooth Disk Surface

The flying height change during track-seeking is mainly due to the HGA inertia and skew angle change. Generally speaking, ABS designs with relatively larger stiffness and larger damping should minimize the inertial effects during acceleration or deceleration. ABS designs that are less sensitive to skew angle change should have a smaller spacing change. Skew angle refers to the angle between the slider's longitudinal axis and the track direction. It's also named as the *geometrical* skew angle. The *effective* skew angle is the angle between the slider's longitudinal direction and the relative disk velocity (or air flow velocity) which is the resultant vector of the disk track linear velocity and the slider's seek velocity. As the seek velocity increases, the difference between the geometrical and effective skew angles increases. Therefore the skew angle effect is more significant during the track-seeking than

during track-following. And this is why such "constant-flying-height" sliders as the TPC and TNPS sliders exhibit significant flying height changes during track-seeking process. They are usually optimized to be insensitive to the geometrical skew angle.

Figure 3 describes the track-seeking profiles used in our study. The simulation starts with an outward seek that is followed by an inward seek, thus completing a whole seeking loop. During the outward seeking process, to move the head from the radial position of 20.48 mm to 33.67 mm, the slider is first accelerated to 2.644 m/s in 4 ms, followed by 1 ms of constant velocity, then it is decelerated to zero velocity in 4 ms. The maximum acceleration is about 67G. During the seek the geometrical skew angle changes from 7.524 degrees to -7.305 degrees. For the inward seek, we simply reverse the outward seeking process. We assume that each process takes 11 ms. Although the actual seeking profile may be different, the major characteristics of track-seeking are contained in the profiles used here.

Figures 4 and 5 illustrate the changes of geometrical skew angles, outer trailing edge flying heights, pitch and roll angles during this complete seeking loop for the TNPS and U sliders. The inertial effect can be clearly seen from the roll and flying height curves in both figures. The start/stop of acceleration or deceleration induces an abrupt roll and hence the flying height changes and subsequent air bearing oscillations. Since the U slider is stiffer than the TNPS slider, the maximum magnitude of flying height and roll changes due to the inertial effect is smaller. However, it takes longer for these oscillations to settle because the U slider has smaller damping.

For most air bearing sliders, the flying height tends to drop as the skew angle deviates significantly from zero [1]. Since the U slider is a negative pressure slider with straight rails, the suspension force is balanced by the net of positive and negative air bearing forces that are both relatively large. As the skew angle changes the balance is quickly lost, which leads to more significant flying height and roll changes. On the other hand, the TPC section of the TNPS slider makes it less sensitive to skew angle change. During the outward seek, for our drive configuration, the effective skew angle decreases initially, therefore the flying height

for both sliders increases for a short period. Since the U slider is much more sensitive to skew angle change, the flying height increase rapidly from 45 nm to 62nm. As the seeking velocity increases, the effective skew angle deviates more from zero. As a result the flying height drops. At the end of the acceleration, the seeking velocity reaches the maximum value, and the effective skew angle thus deviates most from zero. That's where the flying height drops most even though the disk linear speed increases. After that, as the seeking velocity tends to zero, the effective skew angle decreases and converges to the geometrical skew angle. The flying height drop also recovers. For the inward seek, the changes of the flying height, pitch and roll are just the opposite to what happens during outward seek. One interesting observation is that the minimum flying height of the TNPS slider occurs during outward seek and at a radius closer to the OD, which is similar to the behavior of the TPC slider observed in [2] [3], while it occurs during inward seek and at a radius closer to the ID for the U slider. Comparing Figures 4 and 5, we can see that the TNPS slider is a much better design as far as seek performance is concerned.

To investigate the effect of acceleration, we performed the outward track-seeking simulation of the 30% TNPS slider with an increase of the maximum seeking acceleration to 100G. From Figure 6 one can see that, at the start/end of the acceleration the HGA inertia causes the sudden changes of roll angle and hence flying height. And the magnitude of these changes increases with the increase of acceleration. Meanwhile, since the relative disk velocity increase leads to a larger effective skew angle, the flying height drop is much more severe for an acceleration of 100G. Therefore for high performance disk drives with smaller access time, the design of the air bearing slider becomes more challenging.

3.3 Transition from a Laser-Textured Zone to the Data Zone

Recently, a laser texture technique has been developed to reduce the static friction, "stiction", in the head/disk interface during contact startup. These well-placed laser bumps serve as gentle and smooth support points for the contacting slider and hence provide excellent

tribological performance due to low CSS stiction and good durability [14]. How these laser bumps affect the flying of the air bearing slider is of concern, especially when the slider moves from the laser texture zone to the data zone or vice versa. To address this issue, we performed the simulation of a TNPS slider in transition from a laser texture zone to the data zone.

Figure 7(a) is an expanded graphical image of the crater-shaped laser bumps used in this study. For the bump shown in this figure, the rim height is 20 nm and the radius is $20\mu m$. Figure 7(b) is the top-view of part of the numerically generated laser texture zone consisting of crater-shaped laser bumps shown in Figure 7(a). The bumps are 100 μm apart in the tangential direction and 50 μm apart in the radial direction. The laser texture zone starts at disk radius 19.5 mm and ends at 21.5 mm. The blur in the central part of this image is due to the fact that the numerical grids generated in this region (recess area) are relatively coarse.

In Figure 8 we compare the performance of the TNPS and U sliders flying on and off of the laser texture zone. The rim height of the laser bumps is 30 nm and the distribution is as described above. First the sliders fly at the disk radius of 20.48 mm for 0.5 ms, then they are accelerated outwards with an acceleration of 67G. The sudden acceleration leads to a rapid increase of the roll angle and hence a drop of the flying height (at outer trailing edge). Note that the flying heights in Figures 8 and 9 are with respect to the nominal flat disk surface. When the sliders fly off of the laser texture zone, the spacing change of 30 nm causes a quick roll angle change. And the roll angle change of the TNPS slider is larger than that of the U slider, because the U slider has a stiffer air bearing. These roll angle changes recover in about 0.5 ms.

We further investigated the effect of the rim heights of the laser bumps on the TNPS slider. The results are shown in Figure 9. We keep the bumps' radii fixed at 20 μm and use rim heights of 20, 30 and 40 nm. Before the slider reaches the laser texture zone border, the absolute flying height (with respect to the nominal flat disk surface) increases with the

increase of bump rim height. The pitch angle decreases with the increase of the rim height. So does the roll angle. The magnitude of the oscillation of the flying height, pitch and roll (due to the disturbance of the laser bumps) all increase with the increase of the rim height. When the slider flies across the border, the increase of the pitch and roll angles is proportional to the increase of the rim height. The drop of the flying height increases with the increase of bump rim height. For the case of 40 nm bumps, the flying height drop is as large as 4.5 nm.

4 Conclusion

Using the CML's air bearing dynamic simulator, we studied the track-seeking dynamics of two pico sliders on smooth and laser-textured disks. The air bearings of the 30% TNPS and U sliders exhibit distinct dynamic characteristics. The air bearing of the U slider is found to be stiffer than that of the TNPS slider, while the air bearing of the TNPS slider has larger damping ratios. As a result, the magnitudes of the oscillations of roll and flying height due to the inertial force of the seek process are larger for the TNPS slider. But it takes less time for those oscillations of the TNPS slider to damp out. Since the U slider is more sensitive to the skew angle change, the envelop of the flying height during the seeking loop is much larger. An increase of the seeking acceleration leads to more significant inertial effects (larger roll increase at the start of acceleration) and larger spacing change. During transition off of the laser texture zone, the higher the laser bumps, the larger the increase of the roll angle. The stiffer U slider has smaller roll change when moving off of the laser texture zone. A stiffer air bearing is desirable to avoid a potential dynamic instability problem and possible head/disk impact.

5 Acknowledgment

This work is supported by Quantum Corporation and the Computer Mechanics Laboratory at the University of California at Berkeley. We would like to thank Geoff Kaiser and Pete Griffin of Quantum Corporation for their helpful discussion and for providing the slider design data.

References

[1] Berg, L.J. and Buettner, D.C., 1992, "Head/Disk Spacing Changes During Track Accessing in Magnetic Recording Hard-Disk Drives," *Adv. Info. Storage Syst.*, **4**, pp.169-180.

[2] Cha, E. Chiang, C., Lee, J.K., 1995, "Flying Height Change During Seek Operation for TPC Sliders," *IEEE Transactions on Magnetics*, **31**(6), pp.2967-2969.

[3] Liu, B. and Soh, S.H., 1996, "Effects of Seeking Velocity on Air Bearing Skew Angle, Air Flow Speed and Flying Performance of Sliders with Different ABS Designs," *IEEE Transactions on Magnetics*, **32**(5), pp.3693-3695.

[4] Meyer, D.W., "Pico: Why a 30% Form Factor," *IDEMA Insight*, May/June, 1997, pp.3.

[5] Chen,L.-S., Hu, Y. and Bogy, D.B., 1998, "The CML Air Bearing Dynamic Simulator Ver. 4.21," *CML Technical Report*, **97-018**.

[6] Zeng,Q.-H., Chen,L.-S. and Bogy, D.B.,1997 "A Modal Analysis Method for Slider Air Bearings in Hard Disk Drives," *IEEE Transactions on Magnetics*, **33**(5), pp.3124-3126.

[7] Cha, E. and Bogy, D.B., 1995, "A Numerical Scheme for Static and Dynamic Simulation of Sub-ambient Pressure Shaped Rail Sliders," *ASME Journal of Tribology*, **117**, pp.36-46.

[8] Patankar, S.V., 1980, *Numerical Heat Transfer and Fluid Flow*, McGraw-Hill.

[9] Hutchinson, B.R. and Raithby, G.D., 1986, "A Multigrid Method Based on the Additive Correction Strategy," *Numerical Heat Transfer*, **9**, pp.511-537.

[10] Lu, S. and Bogy, D.B., "A Multi-Grid Control Volume Method for the Simulation of Arbitrarily Shaped Slider Air Bearing with Multiple Recess Levels," *CML Technical Report*, **94-016**.

[11] Newmark, N.M., 1959, "A Method of Computation for Structural Dynamics," *Proceedings of American Society of Civil Engineering*, **85**, EM3, pp.64-97.

[12] White, J.W., 1997, "Flying Characteristics of the Transverse and Negative Pressure Contour ("TNP") Slider Air Bearing." *ASME Journal of Tribology*, **119**(2), pp241-248.

[13] Chen,L.-S. and Bogy, D.B., 1997, "A Numerical Study of the Take-Off Dynamics of the TNPS, Tri-K and U Sliders," *CML Technical Report*, **97-012**.

[14] Baumgart, P., Krajnovich, D.J., Nguyen, T.A., and Tam, A.C., 1995, "A New Laser Texturing Technique for High Performance Magnetic Disk Drives," *IEEE Transactions on Magnetics*, **31**, pp2946-2951.

Slider	Flying Height (nm)	Pitch (μrad)	Roll (μrad)
TNPS	43.31	159.20	-5.71
U	45.03	141.38	-10.07

Table 1: Flying attitudes for the TNPS and U sliders

Slider	Vertical (kN/m)	Pitch (mN-m/rad)	Roll(mN-m/rad)
TNPS	843.5	137.7	101.2
U	1020.0	163.7	152.7

Table 2: Comparison of air bearing stiffness

Slider	Mode 1 (kHz)	Mode 2 (kHz)	Mode 3 (kHz)
TNPS	89.2	131.7	145.9
U	102.3	155.5	163.8

Table 3: Comparison of air bearing natural frequency

Slider	Mode 1	Mode 2	Mode 3
TNPS	4.08	2.28	2.18
U	1.38	0.95	1.03

Table 4: Comparison of air bearing damping

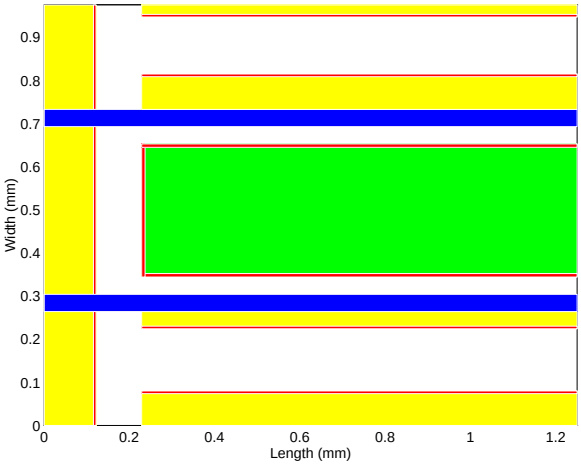

(a) Rail shape

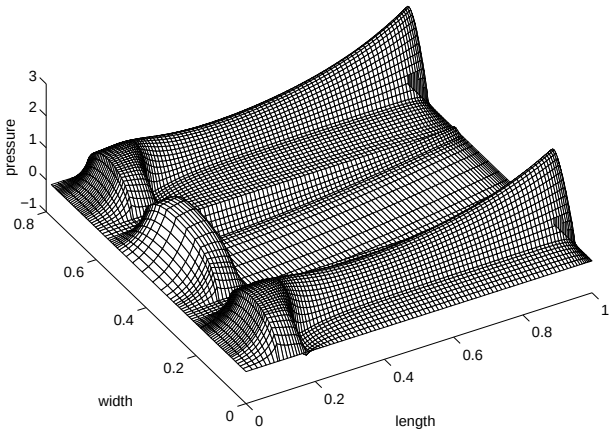

(b) Pressure Profile

Figure 1: Rail shape and pressure profile for 30% TNPS slider

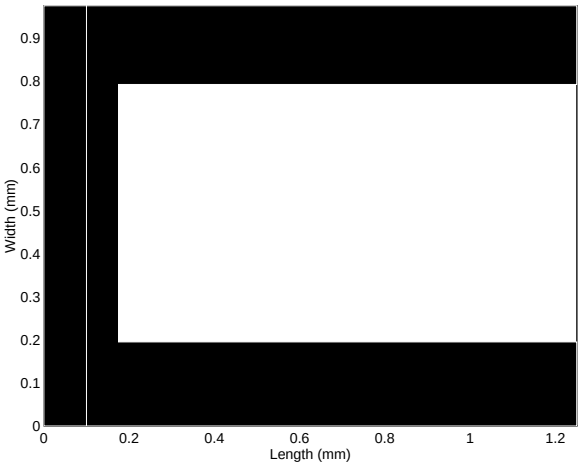

(a) Rail shape

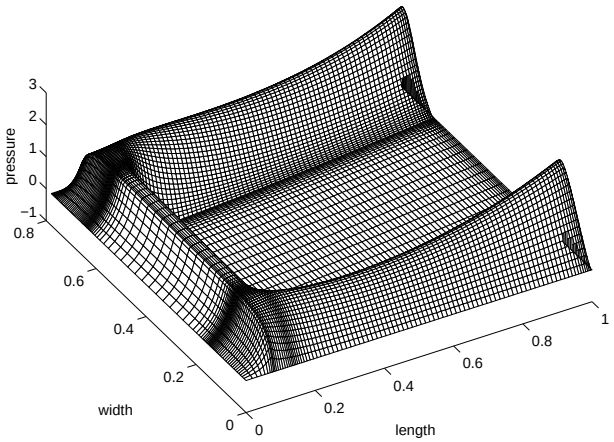

(b) Pressure Profile

Figure 2: Rail shape and pressure profile for 30% U slider

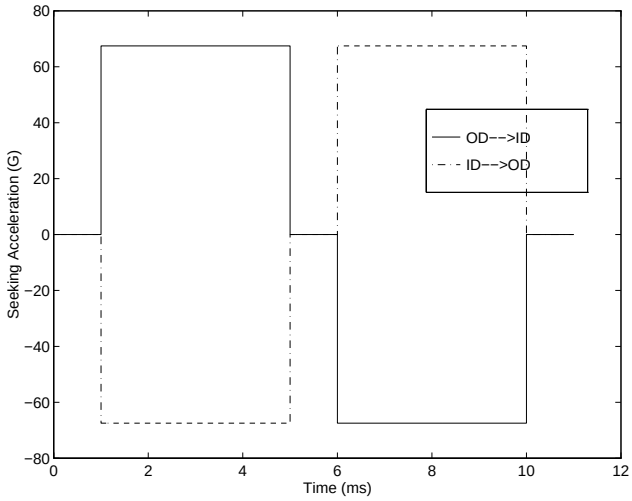

(a) Acceleration history

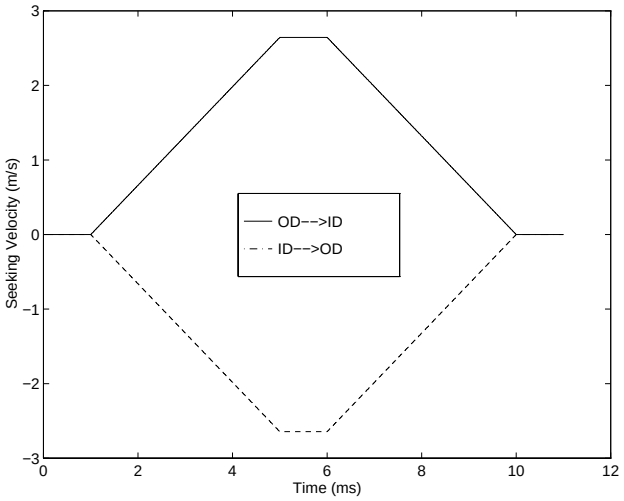

(b) Velocity history

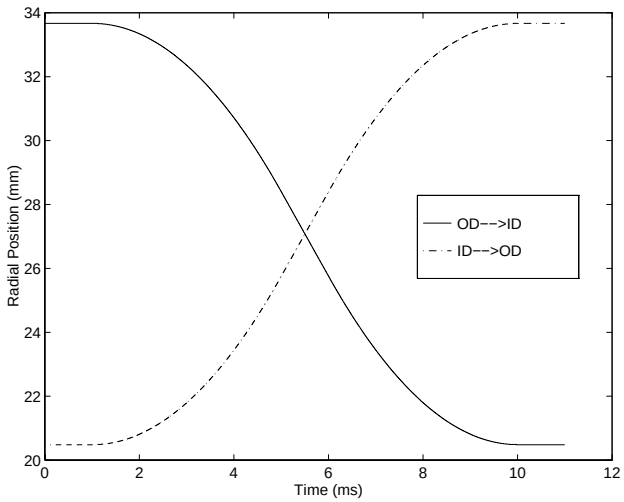

(c) Radial position hisory

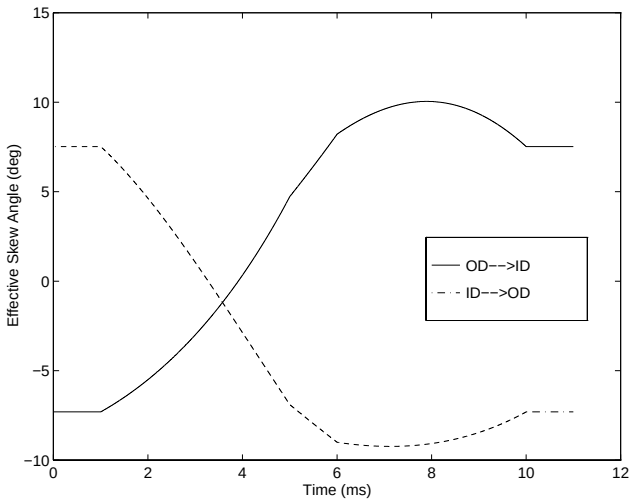

(d) Effective skew angle hisory

Figure 3: Track-seeking history

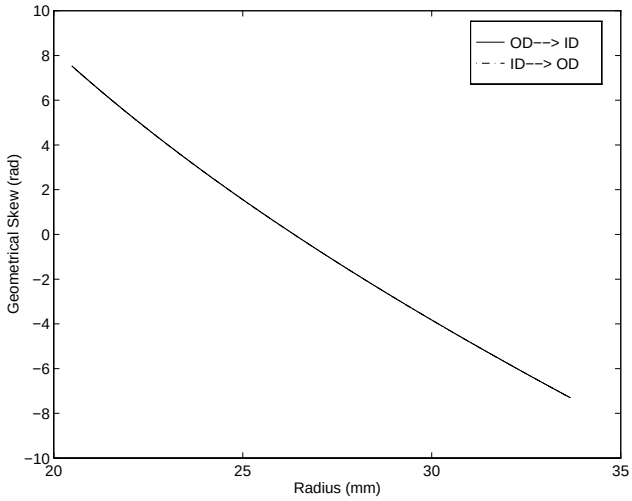

(a) Geometrical skew angle

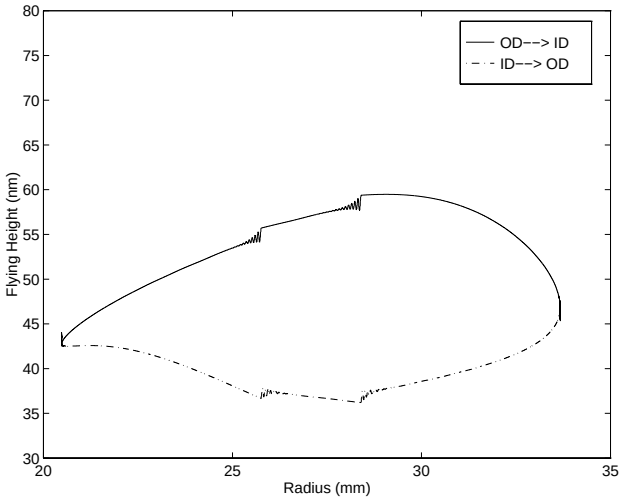

(b) Flying height

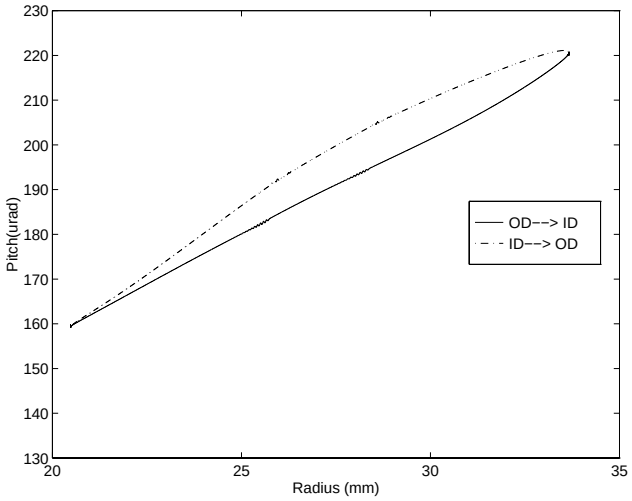

(c) Pitch

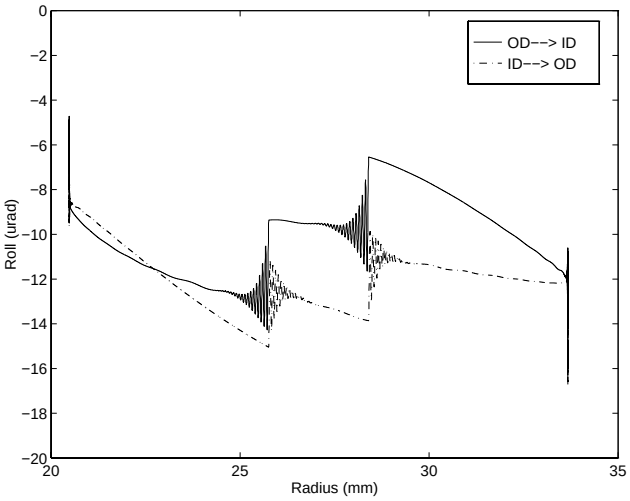

(d) Roll

Figure 4: Track-seeking performance of the TNPS slider

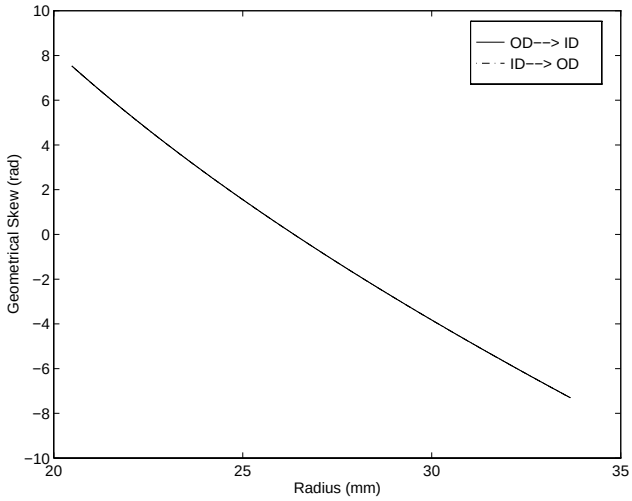

(a) Geometrical skew angle

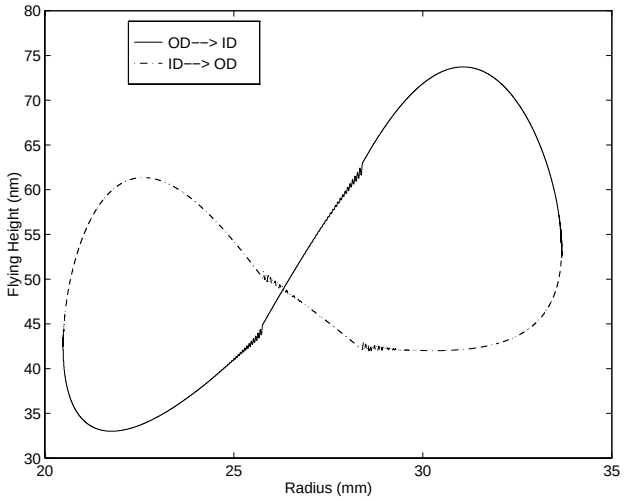

(b) Flying height

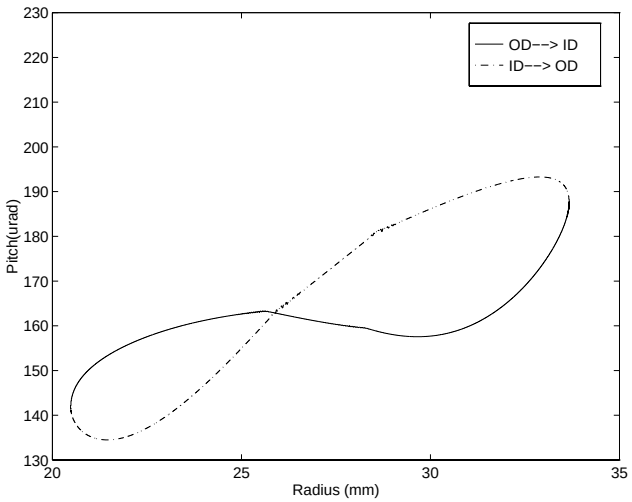

(c) Pitch

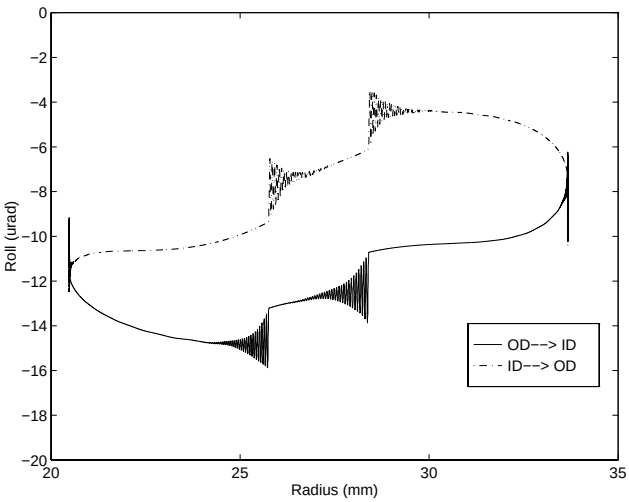

(d) Roll

Figure 5: Track-seeking performance of the U slider

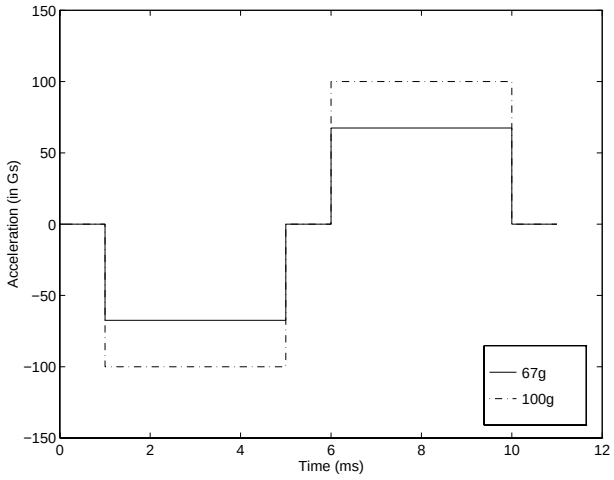

(a) Seeking acceleration profiles

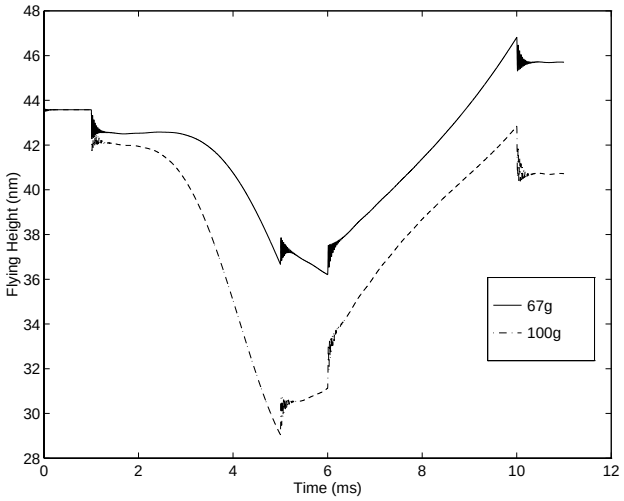

(b) Flying height

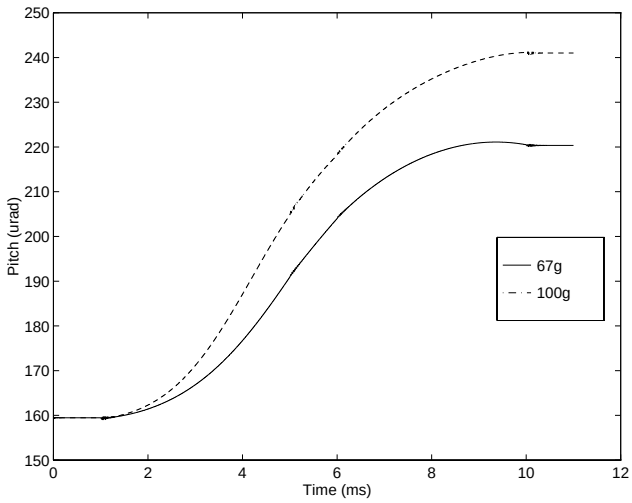

(c) Pitch

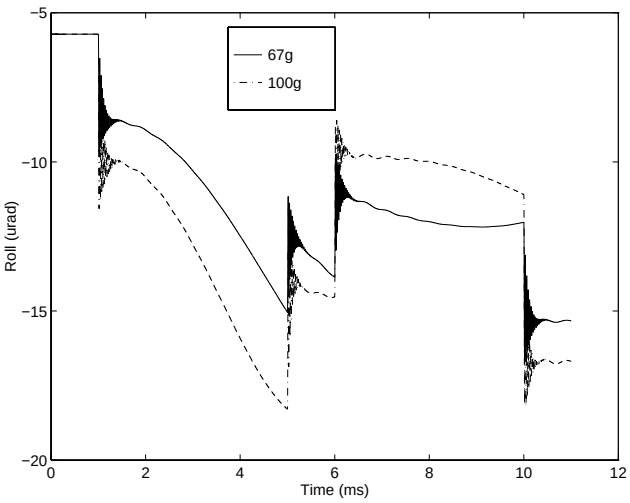

(d) Roll

Figure 6: Effects of seeking acceleration on the performance of the TNPS slider

(a) Laser bump shape (b) Disk topography under the slider

Figure 7: Numerically generated laser bump and laser texture zone

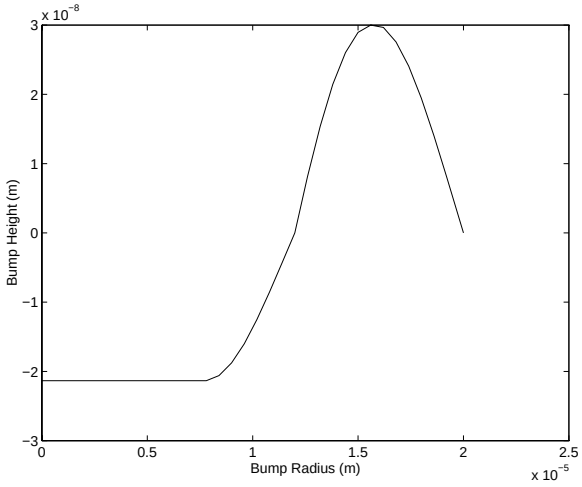

(a) Laser bump shape

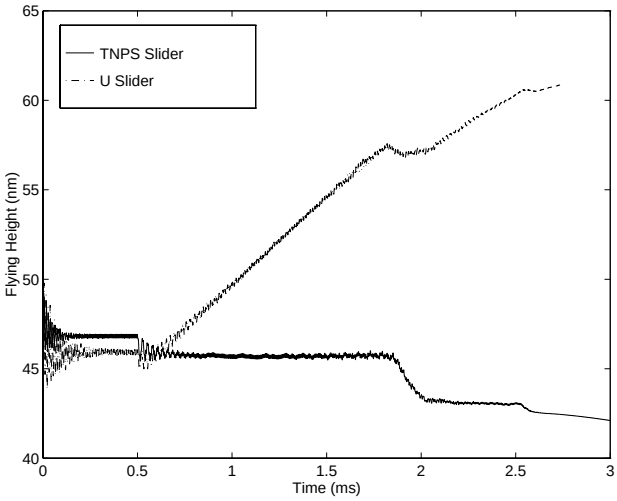

(b) Flying height

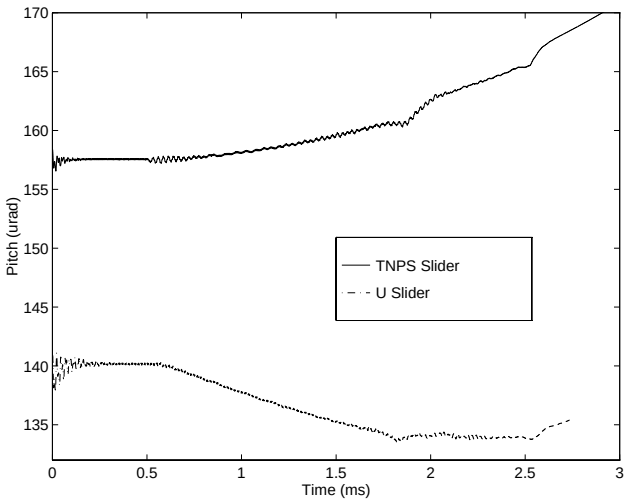

(c) Pitch

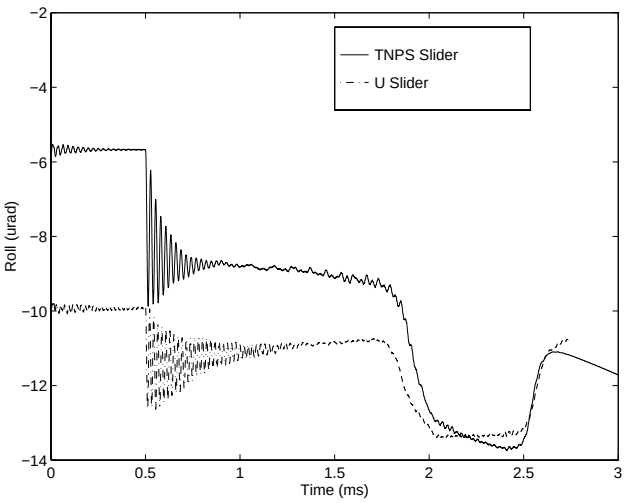

(d) Roll

Figure 8: Comparison of TNPS and U sliders in transition off of the laser texture zone

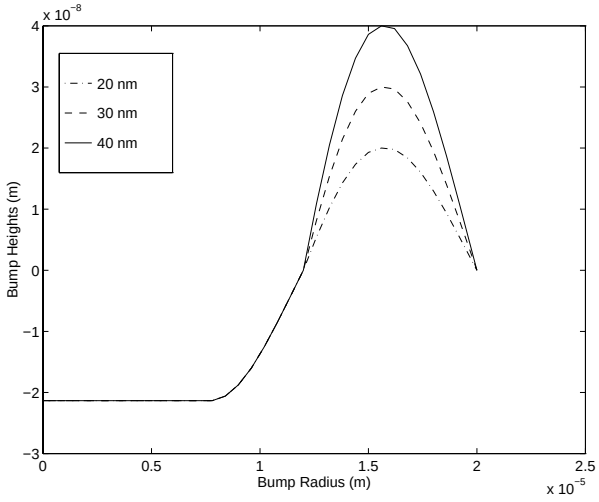

(a) Cross-sectional profile of laser bump

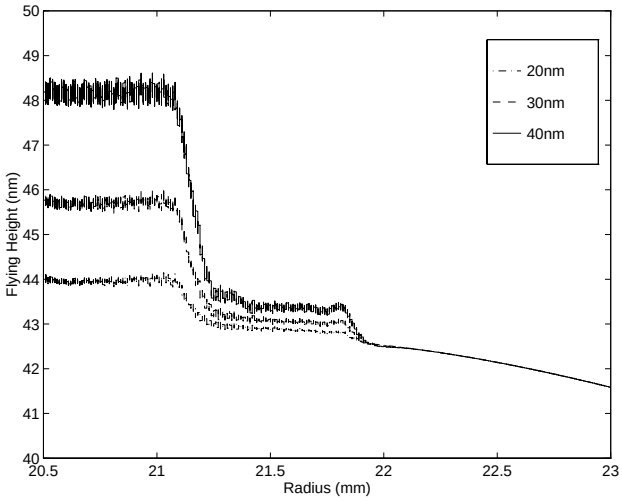

(b) Flying height

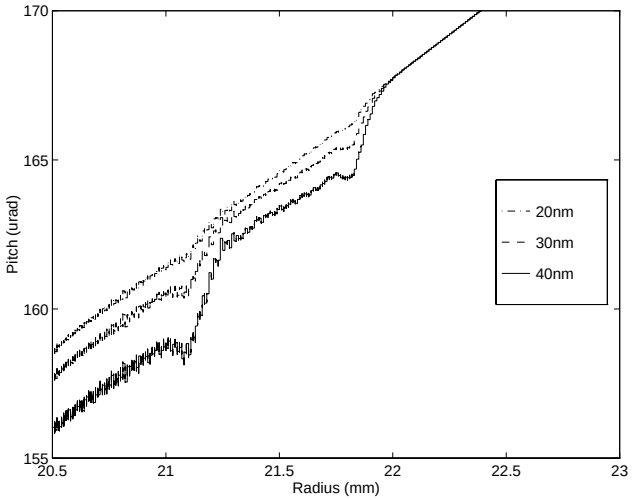

(c) Pitch

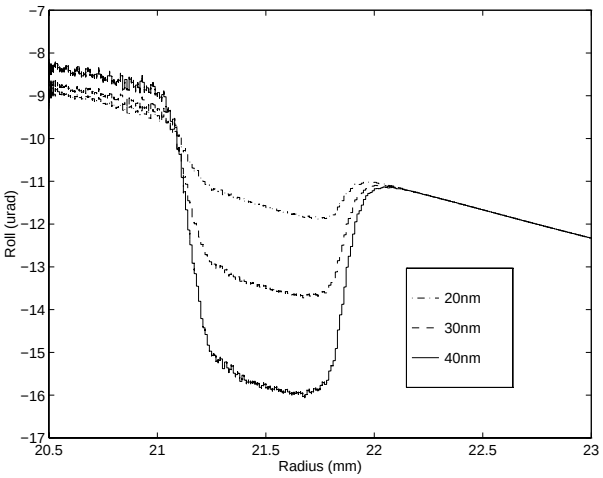

(d) Roll

Figure 9: Effects of laser bump heights on transition of the TNPS slider